Journal of Alloys and Compounds 504S (2010) S159–S162

Contents lists available at ScienceDirect

Journal of Alloys and Compounds

journal homepage: www.elsevier.com/locate/jallcom

Corrosion-fatigue study of a Zr-based bulk-metallic glass in a physiologically relevant environment

Lu Huang[a,b], Gongyao Wang[b], Dongchun Qiao[b], Peter K. Liaw[b], Shujie Pang[a], Jianfeng Wang[a], Tao Zhang[a,*]

[a] Key Laboratory of Aerospace Materials and Performance (Ministry of Education), School of Materials Science and Engineering, Beijing University of Aeronautics and Astronautics, XueYuan Road No. 37, HaiDian District, Beijing 100191, China
[b] Department of Materials Science and Engineering, The University of Tennessee, Knoxville, TN 37996-2200, USA

ARTICLE INFO

Article history:
Received 31 July 2009
Received in revised form 19 January 2010
Accepted 10 February 2010
Available online 18 February 2010

Keywords:
Metallic glasses
Mechanical properties
Corrosion
Scanning electron microscopy

ABSTRACT

Four-point-bend corrosion-fatigue experiments were conducted in a physiologically relevant environment to study the environmental effects on the fatigue behavior of $(Zr_{0.55}Al_{0.10}Ni_{0.05}Cu_{0.30})_{99}Y_1$ (at.%) bulk-metallic glasses (BMGs), and the results were compared with those obtained in air at room temperature. At high stress ranges, the corrosive environment did not significantly affect the fatigue lifetime; while at low stress ranges, the corrosive environment exhibited a detrimental effect on the fatigue resistance. The fatigue strength was decreased by 40% in the physiologically relevant environment. Fracture morphologies after fatigue tests were studied by the scanning electron microscopy. The mechanism for the environmental effects on the fatigue life of the $(Zr_{0.55}Al_{0.10}Ni_{0.05}Cu_{0.30})_{99}Y_1$ BMG was determined to be anodic dissolution.

© 2010 Elsevier B.V. All rights reserved.

1. Introduction

Resulting from their amorphous microstructure, Zr-based bulk-metallic glasses (BMGs) exhibited a unique combination of excellent mechanical and electrochemical properties [1–8], which prompted a great interest in their biomedical applications, especially as medical implants. However, the human body environment is aggressive to implants. The interaction between the corrosive body fluid and the cyclic forces generated by the skeleton system can cause the failure of implants [9]. Thus, as a competitive candidate of implant materials, the corrosion-fatigue behaviors of Zr-based BMGs in a physiologically relevant environment should be investigated.

In this study, the $(Zr_{0.55}Al_{0.10}Cu_{0.30}Ni_{0.05})_{99}Y_1$ (at.%) BMG was selected due to its excellent mechanical properties [1] and good corrosion resistance [4]. Its fatigue behavior in a simulated body environment, which was a phosphate buffered saline (PBS) solution at 37 °C, was investigated and compared with that in air at room temperature (RT). Further, the degradation mechanism for the effects of the corrosive environment, interacting with temperature and cyclic stresses, on the fatigue life was proposed.

2. Materials and experimental methods

Alloy ingots with a nominal composition of $(Zr_{0.55}Al_{0.10}Cu_{0.30}Ni_{0.05})_{99}Y_1$ (at.%) were prepared by arc-melting the mixture of pure elements in an argon atmosphere. Rectangular bars (3 mm × 3 mm × 60 mm) were fabricated by copper-mold casting. The amorphous state of the samples was verified using X-ray diffraction (XRD) within the resolution limits.

Four-point-bend (4PB) fatigue specimens (3 mm × 3 mm × 25 mm) were cut from the as-cast alloy bars, and all four lateral sides were polished to a 1200-grit surface-finish to diminish the effect of surface roughness.

High-cycle 4PB-fatigue tests were conducted in air at RT and in PBS at 37 °C, utilizing a computer-controlled Material Test System (MTS) servohydraulic-testing machine under load control, at a frequency of 10 Hz (sinusoidal waveform) with an R ratio of 0.1, where $R = \sigma_{min}/\sigma_{max}$. ($\sigma_{min}$ and σ_{max} are the applied minimum and maximum stresses, respectively). Corrosion-fatigue tests were conducted in a chamber, containing the PBS solution, which was heated up to 37 °C using a water bath circulating heat coil. Alumina pins were used with inner and outer spans of 10 and 20 mm, respectively. A schematic diagram of corrosion-fatigue configuration was shown in Fig. 1.

To reveal the environmental degradation mechanism, additional corrosion-fatigue tests were conducted with imposed potentials. The electrical connection was enabled by mounting a stainless steel wire to the end of the 4PB-fatigue specimen, using a conductive silver mount. An insulating enamel was applied to both the connection spot and the stainless steel wire to prevent them from the electrolyte. An EG&G Princeton Applied Research 263A potentiostat was employed to control the potential. A saturated calomel electrode (SCE, E_{SCE} = +214 mV) was used as the reference electrode, and two platinum foils were used as counter electrodes. Static polarizations with a cathodic potential of −900 mV and an anodic potential of +900 mV were imposed to specimens, respectively.

Scanning electron microscopy (SEM) was utilized to examine the fracture morphologies on specimens which tested both in air (RT) and in PBS (37 °C).

* Corresponding author. Tel.: +86 10 8233 9705; fax: +86 10 8233 9705.
E-mail address: zhangtao@buaa.edu.cn (T. Zhang).

0925-8388/$ – see front matter © 2010 Elsevier B.V. All rights reserved.
doi:10.1016/j.jallcom.2010.02.080

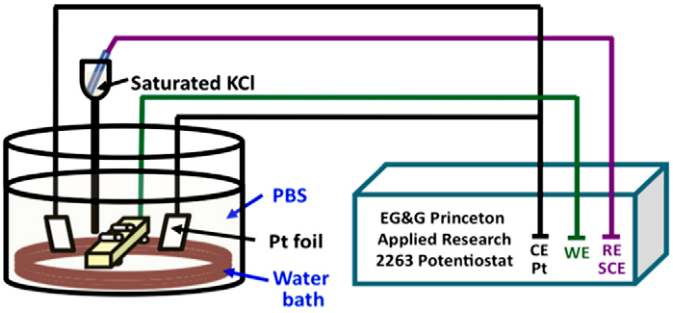

Fig. 1. Schematic diagram of corrosion-fatigue test configuration (loading grips not shown).

3. Results and discussion

3.1. Stress-life behavior

The stress-life behaviors for the $(Zr_{0.55}Al_{0.10}Ni_{0.05}Cu_{0.30})_{99}Y_1$ BMGs tested in air (RT) and in PBS (37 °C) were demonstrated in Fig. 2, by plotting the stress range ($\sigma_r = \sigma_{max} - \sigma_{min}$) as a function of cycles to failure (N_f). At high stress ranges (roughly, $\sigma_r \geq 450$ MPa), the influence of the corrosive environment was not significant, with corrosion-fatigue lifetimes which were comparable to those obtained in air. This is possibly due to that the samples failed within a shorter time at high stresses and the effects of the environment were hindered by the effects of the stresses. However, at low stress ranges (roughly, $\sigma_r \leq 450$ MPa), the environment exhibited a detrimental effect on the corrosion-fatigue lifetimes, which caused fracture at stress ranges that were lower than the fatigue strength found in air (RT). The environment, which was associated with the stresses for a certain time period, initiated corrosion-fatigue failures, the mechanism of which will be explained in Section 3.3. The fatigue strengths in air (RT) and in PBS (37 °C) at 10^7 cycles were 450 MPa (σ_r) and 270 MPa (σ_r), respectively. The environment introduced a decrease of 40% to the fatigue strength in PBS solution (37 °C), as compared to that exhibited in air.

3.2. Fractography

On fatigue specimens that failed in air (RT) and corrosion-fatigue specimens that failed at high stress ranges in PBS (37 °C), fracture initiated on the tension side of the specimen within the inner span, and propagated along the maximum stress plane which was perpendicular to the long axis of the specimen. However, at low stress

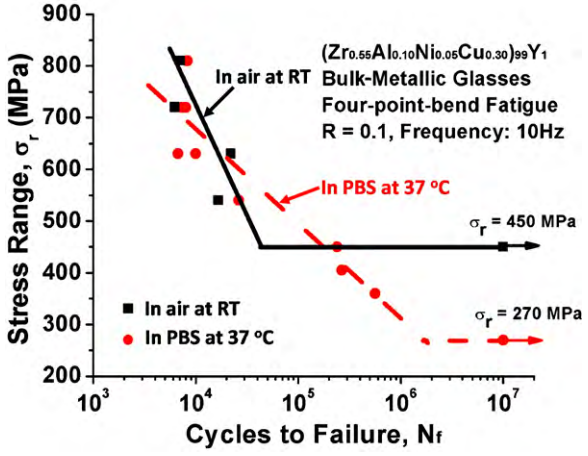

Fig. 2. Stress-life behaviors for 4PB-fatigue tests of $(Zr_{0.55}Al_{0.10}Ni_{0.05}Cu_{0.30})_{99}Y_1$ BMG in air at RT and in PBS at 37 °C.

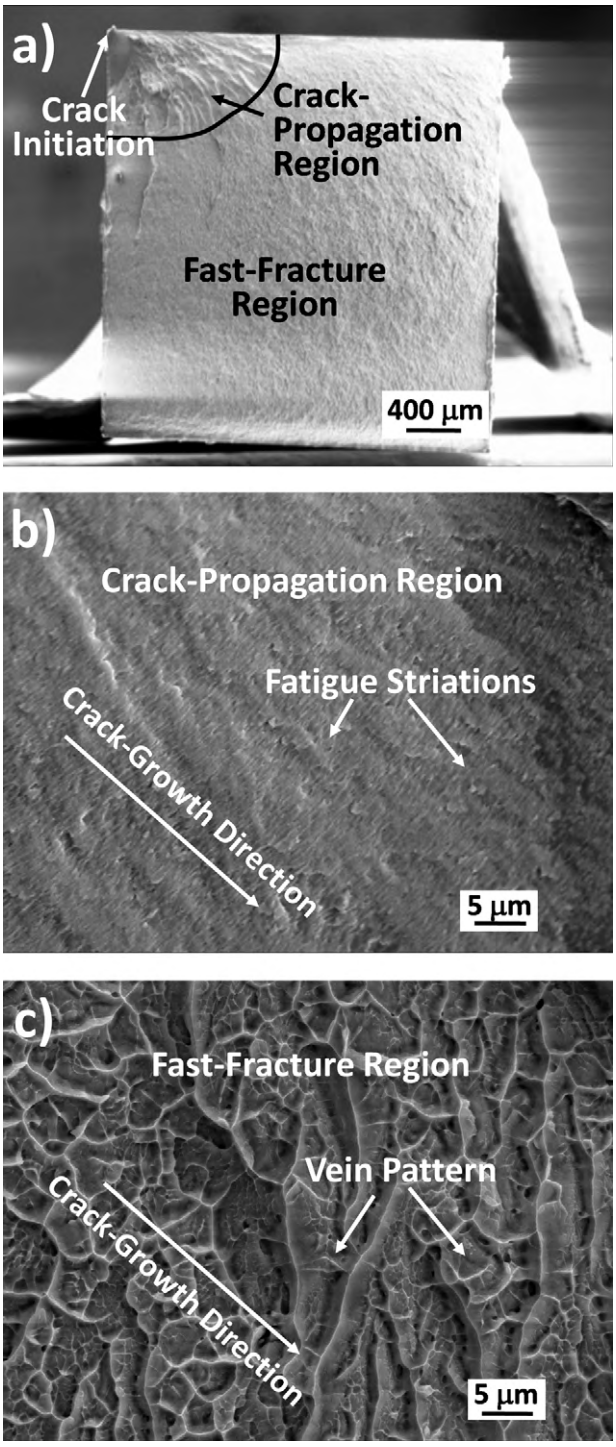

Fig. 3. Fracture morphology of the specimen failed in air (RT) at a stress range of 540 MPa: (a) a mixed morphology of fatigue striations and vein pattern; (b) fine striations; and (c) vein pattern.

ranges in PBS (37 °C), fractures were found not only located within the inner span but also at the outer pins. Some fractures initiated at the outer pin area, and propagated toward the inner pin along a 45° plane to the long axis. The relocation of the fracture initiation could possibly be attributed to the abrasion at the outer pins, which would be explained in Section 3.3.

Fracture morphologies for specimens failed in air (RT) and in PBS (37 °C) were shown in Figs. 2 and 3, respectively. As shown in Fig. 3, the specimen that failed in air (RT) at $\sigma_r = 540$ MPa fractured at the

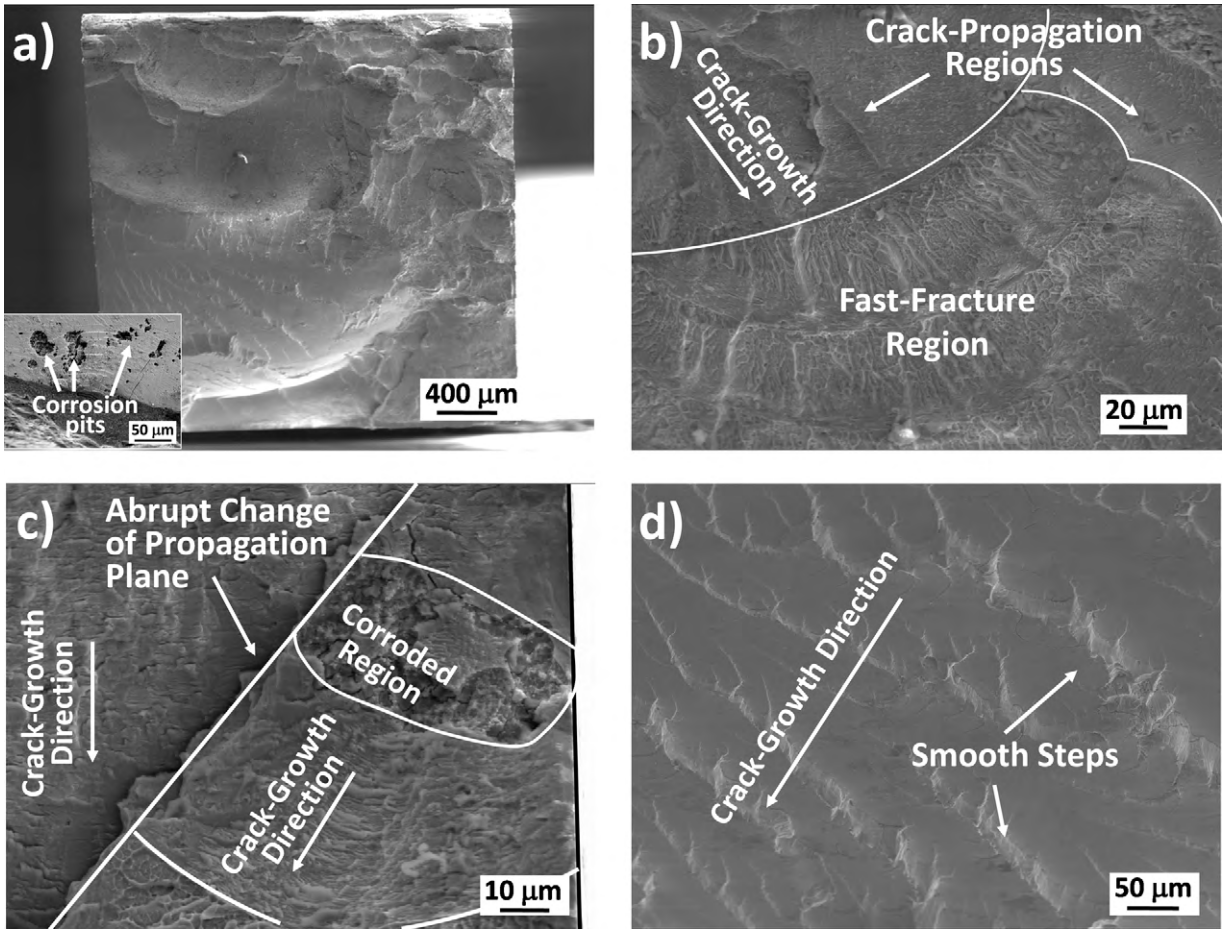

Fig. 4. Fracture morphology of the specimen failed in PBS (37 °C) at a stress range of 360 MPa. (a) A rough fracture surface, (insert: corrosion pits found near the crack-initiation site); (b) crack-propagation and fast-fracture regions; (c) corroded propagation region and abrupt change of propagation plane; and (d) smooth steps.

corner of the tension side of the specimen. The fracture surface exhibited a mixed morphology which was commonly observed on the fracture surface of BMG specimens after fatigue tests [8,10,11], consisted of fatigue striations (Fig. 3b), which represented the crack-propagation region, and the vein pattern (Fig. 3c), which denoted the fast-fracture region.

Specimens tested at high stress ranges in PBS (37 °C) were found to fracture in a similar manner as those tested in air (RT) (not shown). However, at low stress ranges, where the environmental influences became significant, the fracture surface was rougher and more complicated. As shown in Fig. 4, on the specimen that failed in PBS (37 °C) at σ_r = 360 MPa, the fracture exhibited a mixed morphology of not only fatigue striations and vein pattern (Fig. 4b), but also corrosion pits and smooth steps. The crack initiated at the outer pin area where corrosion pits can be observed (see the insert of Fig. 4a). Crack-propagation could be affected by the environmental degradation. Abrupt change of fracture plane was observed on the fracture surface, which was considered to be caused by the degradation at crack tips or propagation frontiers (Fig. 4c), since a corroded region can be observed near the abrupt change. A smooth step-like structure with fine striations on the edges can be observed within the fast-fracture region (Fig. 4d), which, to some extent, implicated a tendency of brittle fracture. This trend is in accordance to that reported by Morrison et al. [6].

3.3. Corrosion-fatigue mechanism

The polarization technique was employed to determine the corrosion-fatigue mechanism. If a cathodic potential increases the fatigue lifetime, the open-circuit degradation mechanism for the corrosion-fatigue behavior is anodic dissolution. While if an applied anodic potential increased the fatigue lifetime, the degradation mechanism is hydrogen-assisted cracking [6,12].

The stress-life behavior for 4PB-fatigue tests of the $(Zr_{0.55}Al_{0.10}Ni_{0.05}Cu_{0.30})_{99}Y_1$ BMG in PBS (37 °C) with and without polarizations was plotted in Fig. 5. Under anodic polarization, the specimen failed quickly after only 5391 cycles, which indicated a decreased lifetime. On the other hand, under cathodic polarization,

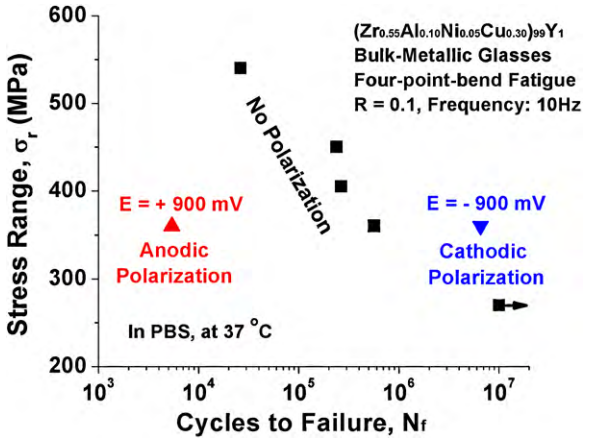

Fig. 5. Stress-life behavior for 4PB-fatigue tests of $(Zr_{0.55}Al_{0.10}Ni_{0.05}Cu_{0.30})_{99}Y_1$ BMG in PBS at 37 °C with and without polarization.

the fatigue lifetime has been increased by more than one magnitude. Thus, it can be concluded that the degradation mechanism for the corrosion-fatigue behavior of the Zr-based BMG in PBS (37 °C) was anodic dissolution.

The degradation process occurred on the specimens failed in the physiologically relevant environment was suggested as follows. When exposed to the electrolyte, a protective passive film was produced on the surface of the $(Zr_{0.55}Al_{0.10}Ni_{0.05}Cu_{0.30})_{99}Y_1$ BMG [4]. However, the abrasion caused by the outer pins or the elastic deformation at the tension side caused by the cyclic force continuously removed or tore the passive film, exposing the underlying metal to the environment. Thus, a corrosion cell formed, with the bare material acting as the anode, and the passive film acting as the cathode, which eased the initiation of pits and made the alloy less corrosion resistant. After the pit initiation, the stress concentrated at the corrosion pit and increased with the growth of the pit and caused the crack-initiation. Anodic dissolution also could happen at a growing crack tip or propagation frontier, and caused the change of the crack-propagation plane, which made the fracture surface rougher.

4. Conclusions

Based on the discussions above, the following conclusions can be made:

(1) At high stress ranges ($\sigma_r \geq 450$ MPa), the environment did not affect the fatigue lifetime of the Zr-based BMG significantly. However, at low stress ranges ($\sigma_r \leq 450$ MPa), the corrosive environment exhibited a detrimental effect on the fatigue resistance. The fatigue strength decreased by 40% in the physiologically relevant environment.
(2) At low stress ranges, environmental degradation influenced crack-initiation, with the assistance of the cyclic force and/or the abrasion of loading pins. Crack-propagation was affected by the environment, which made the fracture surface rougher. A tendency of brittle fracture was observed.
(3) The corrosion-fatigue degradation process for the Zr-based BMG in PBS (37 °C) was proposed, and the degradation mechanism was determined to be anodic dissolution.

Acknowledgements

This work was financially supported by the National Science Foundation (NSF) International Materials Institutes (IMI) Program (DMR-0231320), National Nature Science Foundation of China (Nos. 50771005 and 50631010), National Basic Research Program of China (2007CB613900), PCSIRT (IRT0512) and Program for NCET (NCET-07-0041).

References

[1] J. Luo, H.P. Duan, C.L. Ma, S.J. Pang, T. Zhang, Effects of yttrium and erbium additions on glass-forming ability and mechanical properties of bulk glassy Zr–Al–Ni–Cu alloys, Mater. Trans. 47 (2006) 450–453.
[2] M.Z. Ma, R.P. Liu, Y. Xiao, D.C. Lou, L. Liu, Q. Wang, W.K. Wang, Wear resistance of Zr-based bulk metallic glass applied in bearing rollers, Mater. Sci. Eng. A 386 (2004) 326–330.
[3] G.Y. Wang, P.K. Liaw, M.L. Morrison, Progress in studying the fatigue behavior of Zr-based bulk-metallic glasses and their composites, Intermetallics 17 (2009) 579–590.
[4] L. Huang, D.C. Qiao, B.A. Green, P.K. Liaw, J.F. Wang, S.J. Pang, T. Zhang, Biocorrosion study on zirconium-based bulk-metallic glasses, Intermetallics 17 (2009) 195–199.
[5] S.J. Pang, T. Zhang, H. Kimura, K. Asami, A. Inoue, Corrosion behavior of Zr–(Nb–)Al–Ni–Cu glassy alloys, Mater. Trans. JIM 41 (2000) 1490–1494.
[6] M.L. Morrison, R.A. Buchanan, P.K. Liaw, B.A. Green, G.Y. Wang, C.T. Liu, J.A. Horton, Corrosion-fatigue studies of the Zr-based Vitreloy 105 bulk metallic glass, Mater. Sci. Eng. A 467 (2007) 198–206.
[7] L. Liu, C.L. Qiu, Q. Chen, S.M. Zhang, Corrosion behavior of Zr-based bulk metallic glasses in different artificial body fluids, J. Alloys Compd. 425 (2006) 268–273.
[8] M.L. Morrison, R.A. Buchanan, P.K. Liaw, B.A. Green, G.Y. Wang, C.T. Liu, J.A. Horton, Four-point-bending-fatigue behavior of the Zr-based Vitreloy 105 bulk metallic glass, Mater. Sci. Eng. A 467 (2007) 190–197.
[9] B.D. Ratner, A.S. Hoffman, F.J. Schoen, J.E. Lemons, Biomaterials Science: An Introduction to Material in Medicine, second ed., Academic Press, 2004.
[10] G.Y. Wang, P.K. Liaw, Y. Yokoyama, W.H. Peter, B. Yang, M. Freels, R.A. Buchanan, C.T. Liu, C.R. Brooks, Influence of air and vacuum environment on fatigue behavior of Zr-based bulk metallic glasses, J. Alloys Compd. 434 (2007) 68–70.
[11] D.C. Qiao, P.K. Liaw, C. Fan, Y.H. Lin, G.Y. Wang, H. Choo, R.A. Buchanan, Fatigue and fracture behavior of $(Zr_{58}Ni_{13.6}Cu_{18}Al_{10.4})_{99}Nb_1$ bulk-amorphous alloy, Intermetallics 14 (2006) 1043–1050.
[12] S.A. Shipilov, Mechanisms for corrosion fatigue crack propagation, Fatigue Fract. Eng. Mater. Struct. 25 (2002) 243–259.